Molecules with Multiple Personalities: How Switchable Materials Could Revolutionise Chemical Sensing

F. Benito-Lopez [a], R. Byrne [a], Y. Wu [a,b], L. Nolan [a], J. Kim [a], K-T. Lau [a], G.G. Wallace [b], and D. Diamond [a] *

[a] National Centre for Sensor Research, School of Chemical Sciences, Dublin City University, Dublin 9, Ireland
[b] Intelligent Polymer Research Laboratory, University of Wollongong, ARC Centre of Excellence for Electromaterials Science, Wollongong NSW 2522, Australia.

Worldwide, the demand for sensing devices that can conform with the requirements of large-scale wireless sensor network (WSN) deployments is rising exponentially. Typically, sensors should be very low cost, low power (essentially self-sustaining), yet very rugged and reliable. At present, functioning WSN deployments involve physical transducers only, such as thermistors, accelerometers, photodetectors, or flow meters, to monitor quantities like temperature, movement, light level and liquid level/flow. Remote, widely distributed monitoring of molecular targets remains relatively unexplored, except in the case of targets that can be detected directly using 'non-contact' techniques like spectroscopy. This paper will address the issues inhibiting the close integration of chemical sensing with WSNs and suggest strategies based on fundamental materials science that may offer routes to new sensing surfaces that can switch between different modes of behaviour (e.g. active-passive, expand-contract).

Introduction

Despite the tremendous advances in nanotechnology, which now enables us to manipulate and characterize materials to a level unimaginable to previous generations of sensor scientists, our ability to perform even relatively simple chemical and biological measurements at remote locations is still severely hampered. For example, truly implantable devices capable of long-term (years) chemo/bio-sensing are still unknown, and remote sensing of important chemical and biological targets in the environment is still heavily dependent on platforms that adhere more to the 'coffee-machine' configuration than to the small, autonomous, low-cost devices that could provide dynamic information about the status of our environment at multiple locations (1).

The fundamental problem is that these devices often employ a sensitive sensing surface to generate the chemo/bio-selective signal, and the surface response characteristics are inherently affected by any process that affects the state of the surface-sample interface, such as leaching of receptor molecules (active binding sites), occlusion of the surface (e.g. through bioflouling), or the presence of interferents in the sample. Therefore, this sensitive surface begins to change as soon as it is exposed to the real world, and the response characteristics (slope, selectivity, baseline, response time etc.) also begin to change. Traditionally, analytical scientists have tackled this problem through regular recalibration with standards of known concentration. However, this

means that the device must be capable of sophisticated fluid handling, and must therefore incorporate pumps, valves, reservoirs and conduits for handling of samples and standards. This dramatically pushes up the cost and complexity of the platform, and makes dense deployments of environmental sensors, and long-term implantable sensors fundamentally unrealizable, at least in their present form (2).

Switchable Materials – What can they Offer?

Key challenges that are currently inhibiting more widespread deployments of chemo/bio-sensors in sensor-nets include;

- Highly innovative ways to control liquid movement in microfluidic manifolds that will enable reliable & sophisticated reagent/sample handling in low-cost, low-power devices;
- Strategies to control binding events happening at sensor-sample interfaces; e.g. having surfaces that can be activated/deactivated on demand;
- Integration of features such as referencing, diagnostics and event/artifact discrimination at the molecular level.

We have been working with a number of adaptive or switchable polymers that respond to both electrochemical (e.g. conducting polymers) and optical (e.g. spiropyran modified polymers) stimuli. For example, conducting polymers such as polypyrrole (Ppy) can form the basis of effective soft polymer actuators that can exhibit muscle-like behavior. The actuation effect arises from swelling/contraction that accompanies oxidation and reduction, due to the release/uptake of ions and water of hydration. These polymer actuators can be integrated into microfluidic manifolds in the form of soft polymer pumps and valves, thus providing a route to 'biomimetic' microfluidic circulation systems that are inherently low power, and potentially more reliable in microchannels than equivalent conventional micro-engineered devices (3). Such approaches are important as they could lead to completely new types of biomimetic analytical platforms, that can perform sophisticated functions like sampling, reagent addition, detection, calibration etc., in a compact format, with low-cost fabrication and low power demand. Coupled with low-power wireless communications, the availability of such advanced functions could greatly assist the realization of analytical devices capable of long-term autonomous operation in remote or inaccessible locations (4).

We have also investigated photo-responsive materials, such as spiropyrans derivatives immobilized on polymer substrates (5, 6). These materials exhibit dramatic and reversible changes in properties when illuminated with UV and white light, respectively. UV illumination converts the colorless, uncharged, inactive spiropyran form (SP) to a strongly colored (purple, λ_{max} ca. 560 nm), zwitterionic merocyanine form (MC) that exhibits binding behavior with certain metal ions (7), amino acids (8), organic ions (9) and DNA (10). Upon illumination with white or green light, the active MC form reverts back to the inactive SP form, and typically the bound guest is released. In addition to this photo-reversible binding behavior, the SP, MC and MC-guest forms are also inherently self-indicating, as their colors and UV-Vis and fluorescence spectra are different in each case. These modified polymers therefore can be maintained in an inactive form until requested to convert to the active form (UV exposure); the polymer can then report whether the active form exists (purple color) and whether a particular guest is present via

a further shift of color. The polymer can then be switched back to the inactive SP form using white light, releasing the guest in the process.

Switching between the SP and MC forms can be repeated many times, and we have also demonstrated photo-controlled uptake and release of guest species using SP modified micro/nanobeads (11) Interestingly, SP-modified polymers also exhibit photo-actuation, due to changes in overall charge and solvent uptake/release (12). This can be used to produce photo-switchable polymeric actuators in microfluidic structures (13). Such materials potentially open the way to optically controlled microfluidic manifolds, and to surfaces that can present active (binding) or inactive (non-binding) modes at sensor-sample interfaces. Furthermore, because they exist in more than one form, they are inherently self-referencing, as well as self-indicating. Clearly, these stimuli-responsive materials offer fascinating possibilities for highly innovative approaches to chemo/bio-sensing devices and platforms.

In this paper, we will illustrate the potential of switchable materials to bring new and enhanced capabilities to microfluidic manifolds, which we believe will be critical if next-generation chemical sensing devices are to meet the basic operational requirements of WSN deployments.

Polypyrrole Coated Stainless Steel Mesh (PPy/SSmesh) Valves

Conducting polymers display actuation behaviour under an external redox potential due to the movement of counter ions and associated water of hydration into and out of the polymer, which results in swelling and contraction, respectively. In the oxidized form, the polypyrrole backbone is positively charged, and anions are present in the polymer to ensure charge neutrality. If the polymer is reduced, the anions are expelled along with the water of hydration and the polymer contracts. The opposite effect can be generated through the use of large, lipophilic anions such as dodecylbenzenesulfonate (DBS) which are effectively trapped within the polymer phase, and the predominant charge compensation mechanism is movement of small, mobile cations (and water) in/out of the polymer. These polymer actuators offer intriguing possibilities for building integrated actuator structures within microfluidic manifolds. Intuitively, these might be expected to offer enhanced characteristics compared to valves and pumps based on more conventional engineering approaches employing hard surfaces such as silicon micromachining (14).

To investigate this, we have used a number of strategies. For example, using a stainless steel mesh as a conductive substrate, we have been able to grow PPy over the mesh (15). In this case, the polypyrrole was doped with trifluoromethane sulfonyl imide (TFSI) as this had been previously shown to generate large redox volume changes (8). In addition, the SSmesh had a well-defined regular geometry, which allowed a clear view of the pores opening and closing. Bare SSmesh and fully dried samples of PPy/SSmesh were studied by SEM and typical results are shown in Figure 1. The bare SSmesh has a woven structure, with uniform apertures and filaments around 25 μm in diameter (Figure 1, A). The deposition of PPy produced a relatively uniform increase in the diameter of filament, and gradually filled the pores, eventually leading to complete obstruction (Figure 1, B to D). Close examination showed that the dried PPy was strained, and had a structured surface due to the loss of large content of incorporated liquid. From the

dimensions obtained via the SEMs, the average diameters of PPy coated filament samples were estimated and plotted with respect to the molar density of PPy deposited (Figure 2). As expected, the diameter of the filaments increased with the molar density of PPy until the pores were completely blocked. At this point, the diameter of each filament was ~ 50 μm and the molar density of PPy deposited was 33.1 μmol/cm^2. Further addition of PPy led to the formation of a relatively smooth surface (Figure 1, D). It should be appreciated that the filament diameter of freshly prepared wet PPy/SSmesh samples is larger than that of the dried samples observed using SEM, as the dehydration of the PPy coating during SEM imaging leads to contraction. In-situ optical microscopy confirmed that complete blockage of aperture actually occurred at a molar density < 27.6 μm/cm^2. Therefore, samples with a molar density of 27.6 μmol/cm^2 (Figure 2, labeled with a circle) were used in the following studies.

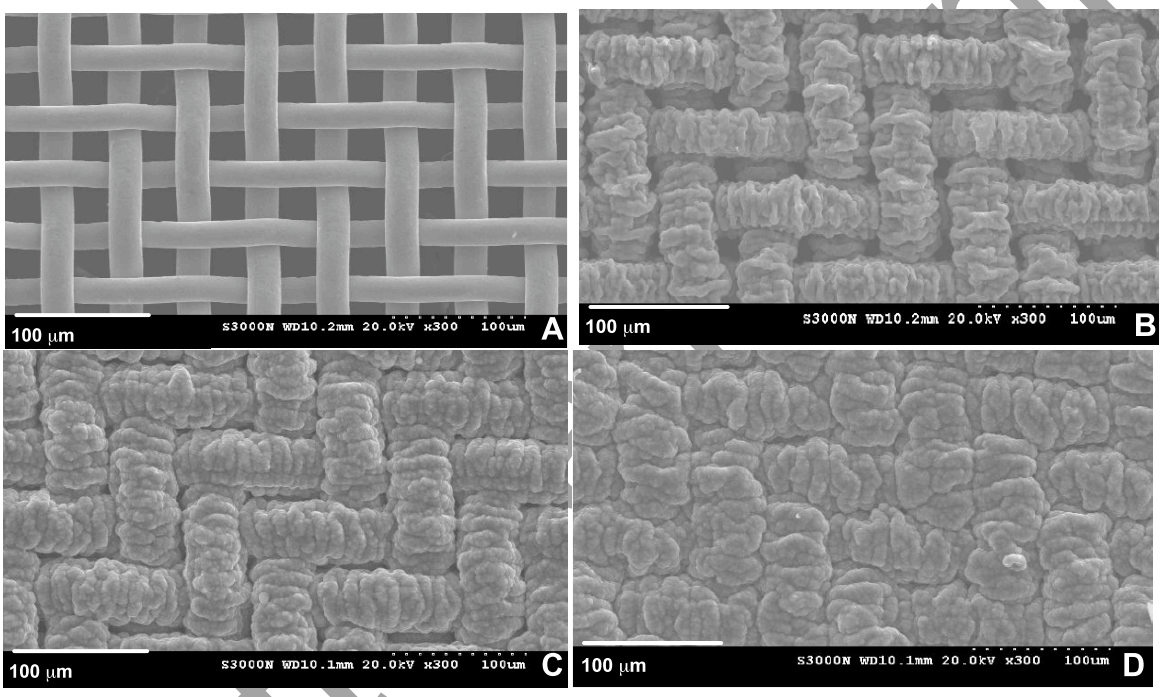

Figure 1. SEM images of dried PPy/SSmesh, (A) the bare SSmesh, (B) PPy at a molar density of 16.5 μmol/cm^2 (C) PPy at a molar density of 27.6 μmol/cm^2 (D) PPy at a molar density of 38.6 μmol/cm^2.

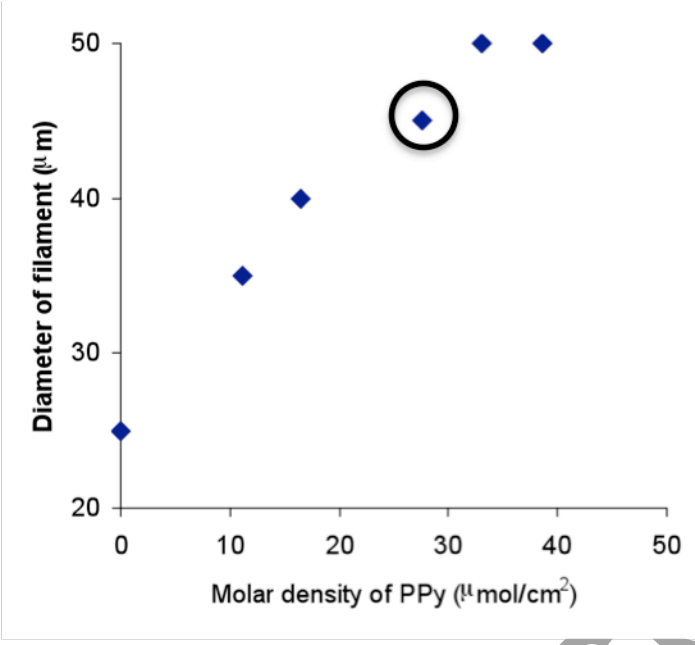

Figure 2. The diameter of the filament of the PPy-coated-SS-mesh increases linearly with the amount of PPy up to a limiting value of ca. 27.6 μmol/cm^2 (see text for explanation).

Cyclic voltammetry (CV) of the PPy/SSmesh

The electroactivity and operational voltage range of the PPy/SSmesh in 0.1 M KCl were determined by CV (Figure 3). Well-defined oxidation/reduction responses were observed at potentials between +/- 0.20 V, indicating that relatively small and mobile counter anions were involved. The peak "A" during the forward scan arises from the oxidation of PPy, and the incorporation of anions/water into the polymer, while peak "B" during the reverse scan arises from the reduction of PPy and the concomitant expulsion of anions/water. In the oxidation potential region, a large change in current was observed at the upper potential limit of +0.60 V when the direction of the potential scan was reversed. This large current indicated that PPy was in a highly conductive form with a large double layer capacitance. Results from CV showed that the freshly prepared PPy/SSmesh was electroactive and the application of potentials between +/- 0.60 V would be sufficient for its complete oxidation and reduction.

Correlation between trans-membrane flow rate and applied potential

The effect of scanning the applied potential between +/-0.60 V on the flow rate of solution across the membrane was examined. The flow rate was monitored by weighing the mass of liquid transferred into a receiving compartment across the membrane as a function of time and converting the mass to a volume (assuming a density of 1 g/mL for the solution). A slow scan rate (1 mV/s) was used in order to minimise diffusion limiting effects on the polymer swelling/contraction, so that changes in the flow rate could be more closely related to the applied potential. Figure 4 shows that the flow rate apparently drifted downwards over time at a relatively constant rate, but superimposed on this was a regular repeating pattern of flow rate variation. Clearly the observed regular variation in

flow rate is related to the triangular applied potential waveform over the range -/+0.60 V, with the maximum flow rate in each cycle coinciding with the minimum applied potential

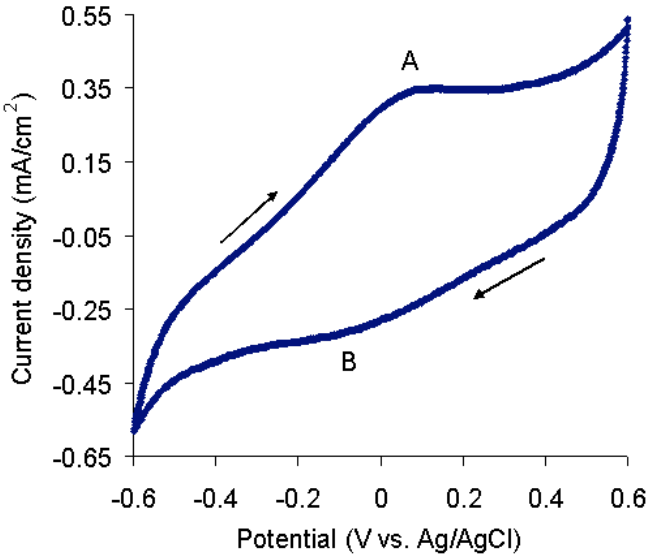

Figure 3. Cyclic voltammogram of PPy/SS mesh in 0.2 M KCl at a scan rate of 1 mV/s

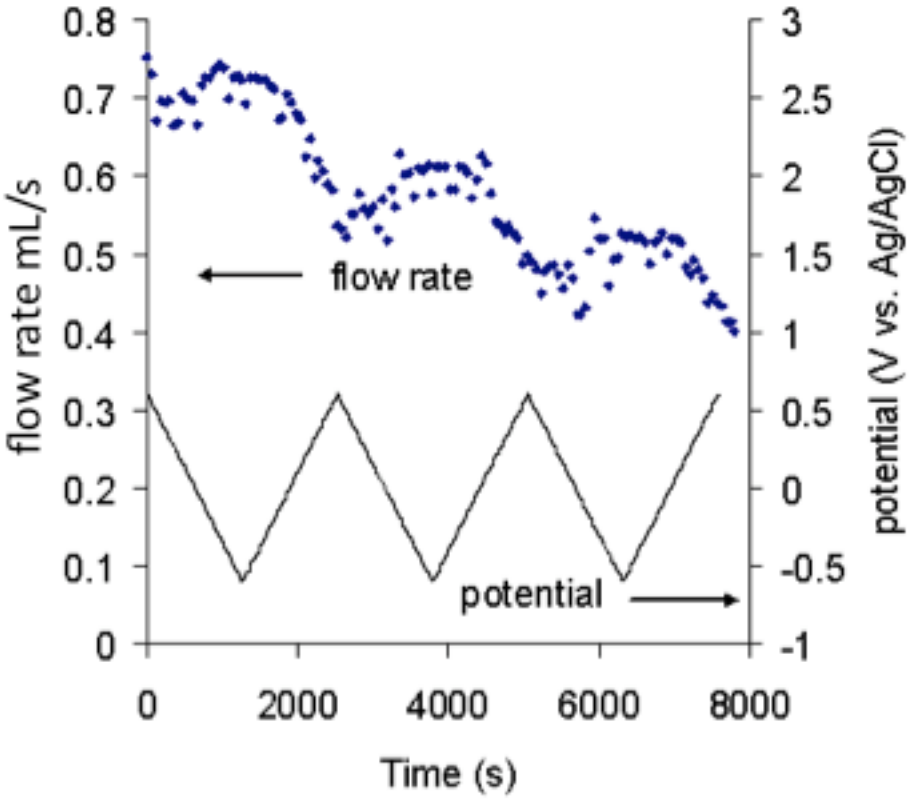

Figure 4. Flow rate changes occurring over the course of several redox cycles of the PPy-polymer mesh structure

and the minimum flow rate coinciding with the maximum applied potential. This can be explained as follows. At oxidative potentials, PPy incorporates counter-anions and associated water, and its volume expands, narrowing the pores and reducing the flow rate. In contrast, at reductive potentials, PPy expels the counter anions and associated water, the polymer contracts, which enlarges the pores and increases the flow rate. The change in flow-rate is non-linear compared to the change in applied potential, with the fastest change was occurring around 0.0 V, which coincides with CV redox peaks (Figure 3), again suggesting that the movement of counter ions is causing this effect.

The linear drift in flow rate (0.14 (mL/s)/minute) observed over the entire duration of the experiment (8000s), is in fact an artifact arising primarily from loss of liquid from the bottom of the liquid column, which provided the head of pressure on the membrane to move transport the liquid across it. Thus as the liquid moved across the membrane from the liquid column, the remaining volume (and hence pressure) decreased, and this affected the flow rate. This was estimated at ~ 5 grams (0.6 mL/s $\times$ 8000s = 4.8 g minus the evaporation of water from the petri dish), which resulted in an applied pressure drop from 4 mBar to 3 mBar across the membrane during the course of the experiment, which resulted in the linear decrease in the observed flow rate. Another contributing factor to this effect is hysteresis in the swelling-contraction cycle, as the polymer does not fully return to its original fully contracted form after expansion. After the drift correction, the maximum change of flow rate induced by redox cycling was 0.15 mL/s, i.e. ~ 20% change in flow rate. These preliminary results show that to some extent, the pore size of the polymer mesh structure can be expanded/contracted, and this effect can be used to regulate the flow rate in a microfluidic channel. With further optimization (e.g. variation of the substrate pore structure, polymer thickness, deposition method, actuation efficiency) clearly this performance can be further improved towards a full on/off effect.

PPy-based Polymer Pumps

Using a laminate-type structure, it is possible to build so-called polymer 'benders'. These typically consist of two PPy-layers that sandwich a flexible porous central layer. The electrical contacts to the PPy layers are such that when one is oxidized, the other is reduced and there is a net transfer of electrolyte and water across the flexible porous middle layer, so that as one layer expands the other simultaneously contracts, resulting in a bending effect (16). Figure 4 shows these bending membranes **2** built into a dual-channel micropump, so that the bending effect can be used to push liquid through the device from a small reservoir **1** to an external port **3**. The sequence of stills from a short video clip shows a droplet forming (top), detaching (middle) and falling onto a tissue (bottom) during an actuation cycle of the pump. Similar effects have been demonstrated using other electroactive polymers (17).

Cleary, these polymer actuators can form the basis of successful biomimetic-type pumps that can be integrated with microfluidic manifolds, and these soft, low-power actuators, do have advantages over conventional micromachined pumps, as mentioned previously. However, they still are very much at the 'proof-of-principle' stage, and to our knowledge, no commercial devices of this type are currently available. This is probably linked to issues such as limited lifetime, relative inefficiency in terms of conversion of electronic

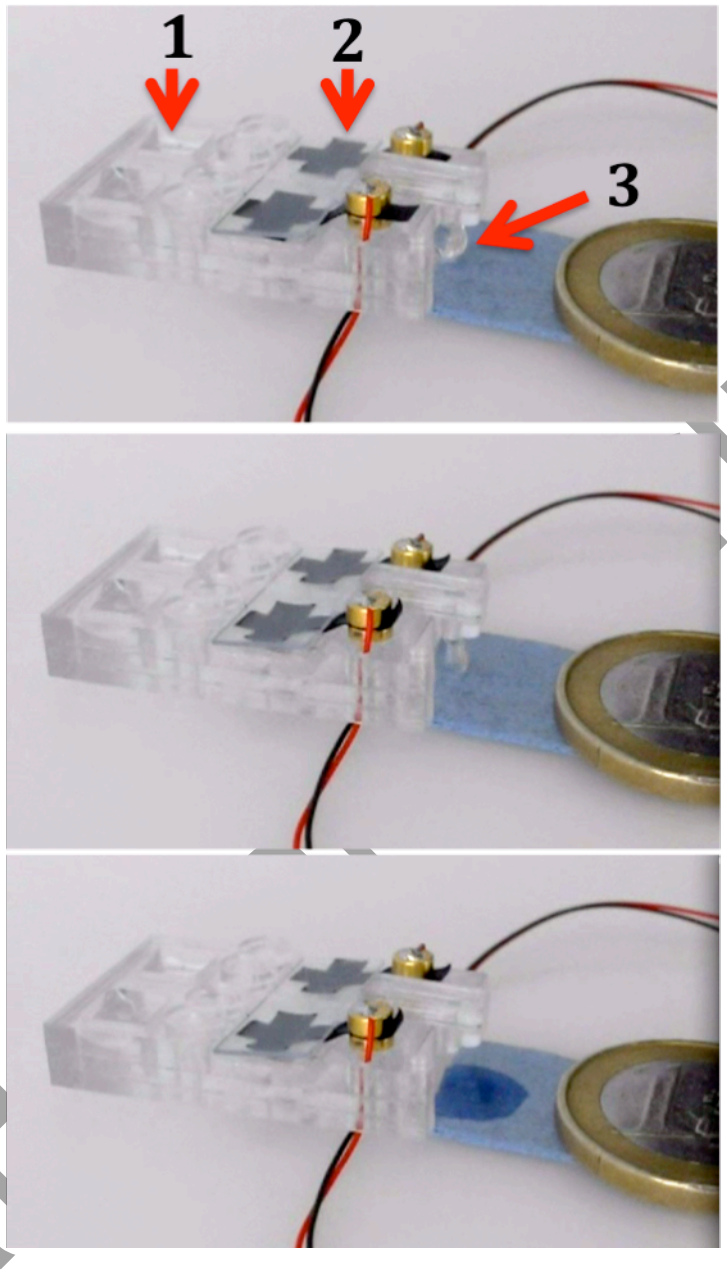

Figure 5. Operation of PPy-based dual channel pump. Flexing of the polymer structures **2** drives water from a reservoir area **1** to an external connector **3**. The sequence shows the formation and release of the droplet generated by the polymer pump.

energy input into mechanical energy output, and the characteristic pulsed-form of the flow. However, this is a very active area of research, and advances are happening continuously in terms of overall efficiency. Furthermore, highly precise and reproducible flow rates are not required for many sensing applications and it can be predicted that devices incorporating polymer actuator pumps and valves will be increasingly employed for niche applications.

Optically Switched actuators

The previous section illustrated how liquid movement can be generated and modulated using electro-active polymer structures built into channels. Compared to existing approaches to fabricating pumping and valving structures based on hard-engineered surfaces (e.g. using silicon micromaching), these structures are more biomimetic in nature, and are potentially more compatible with microfluidic structures, and resistant to micro-particulates that may enter the fluidic system. However, like all electronically actuated devices, they require intimate contact between the source of the actuation stimulus and the actuator; i.e. electronic connectors must be incorporated into the fluidic manifold, and the intimate contact maintained through out the operational lifetime of the device.

Obviously, as devices are scaled down, and become more complex, and incorporate more actuator structures, fabrication issues and reliability become increasingly limiting. In this scenario, optical switching becomes more attractive, as there is no need for a direct physical contact between the stimulation source and the actuator. Bearing in mind the mechanism of swelling/contraction in electroactive polymers (i.e. movement of charged ions and associated water of hydration in/out of the polymer), similar effects may be expected from photoswitchable polymers that undergo significant changes in their charge when exposed to light.

Spiropyran is one such system, as it changes from an uncharged spiropyran form, to a highly charged zwitterionic merocyanine form when exposed to UV-light. This process can be reversed using white light. As mentioned previously, it has been shown that spiropyran modified polymer surfaces show photocontrolled binding of a range of guest species, such as metal ions, amino acids and DNA. Furthermore, the system is self-indicating, as striking changes in colour and fluorescence accompany binding, and switching between the passive spiropyran and active (binding) merocyanine forms (18).

It has been shown that these changes in charge can be used to make polymers that swell and contract upon exposure to light. These effects can be considerably enhanced through the incorporation of ionic liquids in the polymer (19). The resulting ionogels exhibit very dramatic actuation behaviour, and enhanced actuation kinetics. Figure 6 (top) shows a typical formulation used to produce these photoswitchable polymer actuators. It consists of three monomeric units; poly(N-isopropylacrlamide), N,N-methylene-bis(acrylamide) and acrylated benzospiropyran (20) in the ratio 100:5:1, respectively. A reaction mixture solution was prepared by dissolving the NIPAAm monomer, acrylated spirobenzopyran monomer and the photo-initiator DMPA in 1-buthanol. The liquid mixture was deposited into previously formed micro-reservoir structures within a microfluidic manifold and photo-polymerised in-situ within an ionic liquid matrix using UV irradiation. In this example, the ionic liquid matrix used was trihexyltetradecylphosphonium dicyanoamide [P6,6,6,14][dca] (Figure 6). When the polymerization was completed, the ionogel structures were washed with ethanol and HCl aqueous solution to remove the unpolymerised liquid and the excess ionic liquid. They

were then kept for two hours in 0.1 mM HCl aqueous solution, whereupon the ionogel exhibits a drastic and rapid swelling effect, which effectively blocks the microfluidic channel and prevents liquid movement.

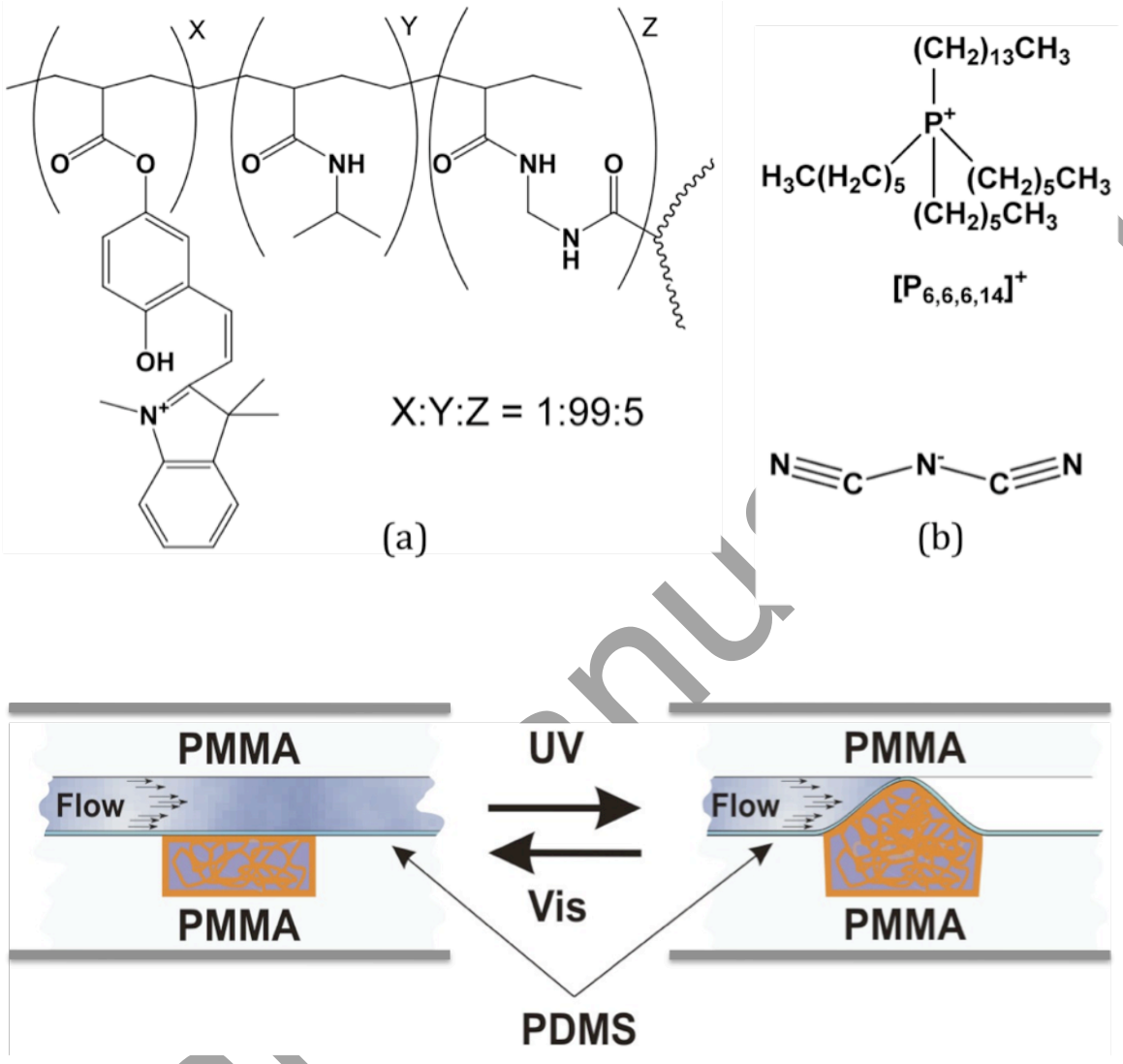

Figure 6. (top) (a) Photo-responsive polymer poly(N-isopropylacrylamide), N,N-methylene-bis(acrylamide) and acrylated benzospiropyran in the ratio 100:5:1, respectively; (b) trihexyltetradecylphosphonium dicyanoamide $[P_{6,6,6,14}][dca]$ ionic liquid chemical structure. (Bottom) The ionogel structure in the contracted form allows liquid to pass through the microfluidic channel (left) but in the expanded form (right) it completely occludes the channel and prevents liquid movement. Switching between the expanded and contracted forms can be achieved using UV or Visible light.

The response of the ionogel valve structure to visible light is demonstrated in figure 7. A droplet of coloured dye is placed in a reservoir at one end of a channel and a vacuum applied to the distal end. At t = 0 s, the photo-valve prevents transport of the liquid through the channel. Exposure of the valve to white light via a fibre-optic probe causes contraction of the ionogel and liquid movement occurs within a few seconds. Controlling liquid movement through channels using light is an exciting development as it potentially

opens the way to very low cost, yet sophisticated fluidic handling platforms, as there is no need for the integration of electronic tracks. Coupled with optical detection this means that the fluidic manifolds could be much easier to make and seal.

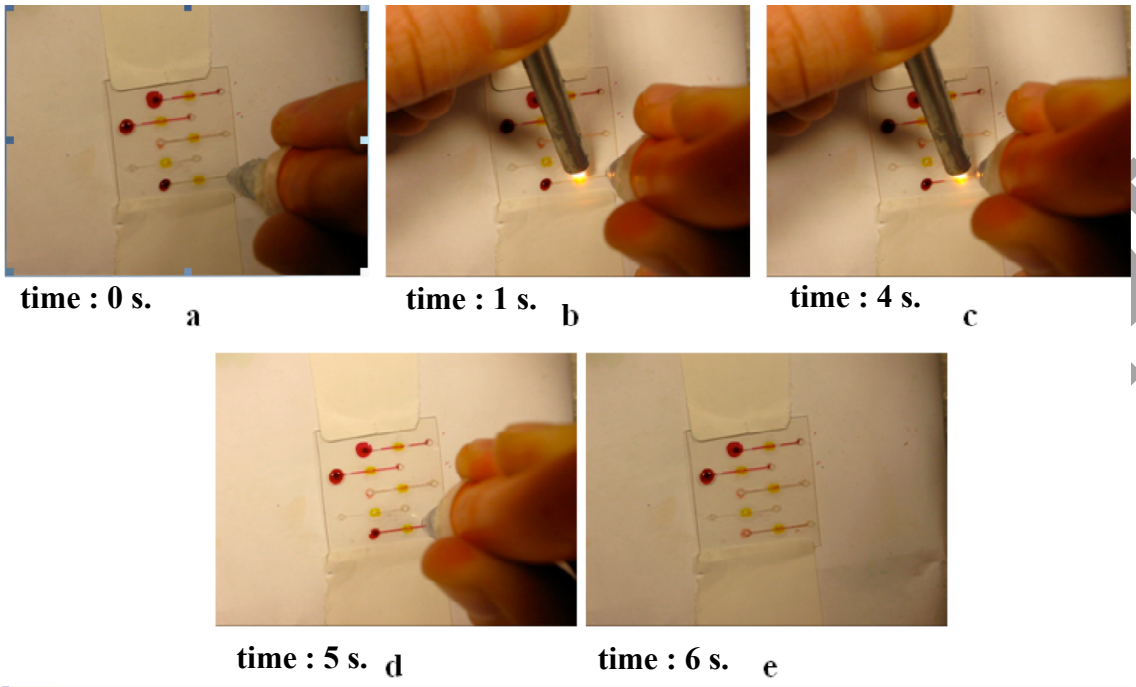

Figure 7. Performance of the ionogel micro-fluidic valve. a) Micro-valve is closed; vacuum is unable to draw the red dye through the micro-channel. b) White light is applied to the valve, causing the ionogel to contract. c-e) The valve is open and the red dye moves through the micro-channel.

Conclusions

In this paper we have shown how it is possible to incorporate polymer actuators into fluidic structures that could provide functions such as sampling, reagent addition, calibration, within an integrated, biomimetic, low-power, low-cost analytical platform. Such developments are crucial for the realization of next generation analytical devices that must combine reliability, ruggedness, self-sustaining character and low cost of ownership with high quality analytical performance. It is only through such developments that chemical sensing can become ubiquitous through society, in the way that transducers have already done. Fundamental breakthroughs in materials science are required to make this happen. The strategies presented here suggest ways of moving forward, but there is no doubt that much work remains to be done before practical devices are realized. Although we can only hint at the intriguing possibilities offered by switchable materials, it is clear that the intersection between fundamental materials science, chemical sensing, and wireless communications will be an exciting field of research for the foreseeable future.

Acknowledgments

We acknowledge financial support for aspects of this research from Science Foundation Ireland (CLARITY CSET award 07/CE/I1147), Australian Research Council (ARC) Linkage Award, IRCSET Fellowship number 2089 for F B-L, and the Biotex FP6 project for YW. GGW is grateful to the ARC for funding in the form of a Federation Fellowship.

References

1. D. Diamond, *Analytical Chemistry*, **76**, 278A-286A (2004).
2. D. Diamond, S. Coyle, S. Scarmagnani and J. Hayes, *Chemical Reviews*, **108**, Issue: 2 652-679 (2008).
3. S. Ramirez-Garcia and D. Diamond, *Journal of Intelligent Material Systems and Structures*, **18** (2), 159-164 (2007).
4. D. Diamond, K-T. Lau, S. Brady and J. Cleary, *Talanta* **75**, 606-612 (2008).
5. S. Stitzel, R. Byrne and D. Diamond, *J. Mater. Science*, **41,** 5841–5844 (2006).
6. R. Byrne, S. E. Stitzel and D. Diamond, *J. Mater. Chem*. **16**, 1332-1337. (2006).
7. A. Radu, S. Scarmagnani, R. Byrne, C. Slater, K-T. Lau and D. Diamond, *J. Phys.D; Appl. Phys.*, **40**, 7238-7244 (2007).
8. R. Byrne and D. Diamond, *Nature Mater*., **5**, 422-424 (2006).
9. R. Byrne, K. J. Fraser, E. Izgorodina, D.R. MacFarlane, M. Forsyth and D. Diamond, *Physical Chemistry Chemical Physics*, **10**, 5919-5924 (2008**)**
10. J. Andersson, S. Li, P. Lincoln, and J. Andreasson, *JACS* ,**130**, 11836–11837 (2008).
11. S. Scarmagnani, Z. Walsh, C. Slater, N. Alhashimy, B. Paull, M. Macka and D. Diamond, *J. Mater. Chem*., **18**, 5063 – 5071 (2008).
12. K. Sumaru *Chem. Mater.,* **19** (11), 2730 -2732 (2007). A. Szilagyi, K. Sumaru, S. Sugiura, T. Takagi, T.Shinbo,M. Zrinyi and T. Kanamori, *Chem. Mater.*, **19**, 2730-2732 (2007).
13. S. Sugiura, K. Sumaru, K. Ohi, K. Hiroki, T. Takagi and T. Kanamori, *Sensors and Actuators A*, **140**, 176–184 (2007).
14. S. Ramırez-Garcia, M. Baeza, M. O'Toole, Y. Wu, J. Lalor, G. G. Wallace and D. Diamond, *Talanta*, **77**, 463–467 (2008).
15. Y. Wu, L. Nolan, S. Coyle, K-T. Lau, G. G. Wallace and D. Diamond, *Proceedings of the 29th Annual International Conference of the IEEE Engineering in Medicine and Biology Society*, Lyon, France, 22-26 August 2007, 4090-4091.
16. C. Smyth, K-T. Lau, R. L. Shepherd, D. Diamond, Y. Wu, G. M. Spinks and G. G. Wallace, *Sensors and Actuators B*, **129**, (2) 518-524 (2008).
17. S. Ramırez-Garcıa and D. Diamond, *Sensors and Actuators A*, **135**, 229–235. (2007).
18. R. Byrne, A. Radu, N. Alhashimy, C. Slater, W. S. Yerazunis and D. Diamond, *Proceedings of the European Coatings Conference 'Smart Coatings V'*, Berlin, Germany, May 15th and 16th 2006, pp. 65-76.
19. F. Benito-Lopez, R. Byrne, A. M. Raduta and D. Diamond, *manuscript in preparation*.
20. K. Sumaru, K. Ohi, T. Takagi, T. Kanamori, T. Shinbo, *Langmuir*, **2**, 4353-4356 (2006).